DOI: 10.1002/ejic.200600058

Study on the Photochromism of Ni–Al Layered Double Hydroxides Containing Nitrate Anions

Min Wei,[a] Xiangyu Xu,[a] Xinrui Wang,[a] Feng Li,[a] Hui Zhang,[a] Yanluo Lu,[a] Min Pu,[a] David G. Evans,[a] and Xue Duan*[a]

Keywords: Layered compounds / Photochromism / Host–guest systems

The photochromism of nitrate-containing nickel–aluminum layered double hydroxides (NiAl-NO_3-LDHs) has been studied. Powder X-ray diffraction (PXRD), FTIR, UV/Vis, XPS, ESR, EXAFS, and elemental analysis were used to investigate the structure, composition, and photochromic behavior of NiAl-NO_3-LDHs. A possible photochromic mechanism in NiAl-NO_3-LDHs has been proposed.

Introduction

Layered double hydroxides (LDHs) consist of metal brucite type layers – $Mg(OH)_2$ sheets where octahedra of Mg^{2+} ions, sixfold coordinated to OH^-, share edges to form two-dimensional infinite sheets. LDHs constitute a vast family of compounds of general formula $[M^{II}_{1-x}M^{III}_x(OH)_2]A^{y-}_{x/y}\cdot nH_2O$, where x typically varies between 0.20 and 0.33. They are stacks of positively charged, partially substituted brucite-like layers that are spaced by exchangeable A^{y-} anions and water molecules.[1,2] LDHs are attractive materials for various fields of application such as catalysis,[3] optical materials,[4,5] biomimetic catalysis,[6,7] separation science,[8,9] medical science,[10,11] and electrochemistry.[12,13]

Recently, research on photochromic materials has received much attention because of the potential use of these materials in photonic applications. Practical applications are also well established, for example, in optical transmission.[14] Photochromism is also widely utilized from the molecular level up to complete devices; representative examples are molecular switching of host–guest aggregates,[15,16] sol–gel thin films,[17] and pigment–protein complexes involved in proton pumping.[18] However, there are very few reports of LDHs being used as candidates for photochromic materials. It has been reported that a sulfonated spiropyran dye (SP-SO_3^-) intercalated in Mg–Al, Zn–Al, and Li–Al LDHs exhibited photochromism due to interlayer reversible photoisomerization between SP-SO_3^- and photoinduced merocyanine.[19,20]

Although photochromism resulting from the properties of the interlayer organic guest has been observed in LDH composites, the mechanism related to the host–guest interaction has not been reported. In this paper, we report for the first time photochromism in a NiAl-NO_3-LDH. PXRD, FTIR, UV/Vis, ESR, XPS, EXAFS, and elemental analysis were used to investigate the photochromic behavior, and its possible mechanism has also been proposed.

[a] State Key Laboratory of Chemical Resource Engineering, Beijing University of Chemical Technology,
Beijing 100029, P. R. China
E-mail: duanx@mail.buct.edu.cn

Results and Discussion

The Crystalline Structure and Chemical Composition of NiAl-NO_3-LDHs

Figure 1 shows the PXRD pattern for NiAl-NO_3-LDHs. A typical PXRD pattern was found for NiAl-NO_3-LDHs prepared by a hydrothermal method (a profile similar to those observed in hydrotalcite-like compounds): sharp and symmetric peaks related to 00l reflections and broad and less symmetric peaks related to 0kl reflections (Figure 1). The peaks were indexed in a hexagonal cell with rhombohedral symmetry, where c = 26.79 Å and a = 3.00 Å. The d_{003} parameter, which corresponds to an interlayer distance of 8.93 Å, is typical for hydrotalcite-like materials containing nitrate anions.[2]

On the basis of elemental analysis, the chemical composition of this particular NiAl-NO_3-LDH (Ni/Al = 2) was found to be $[Ni_{0.643}Al_{0.357}(OH)_2](NO_3^-)_{0.357}\cdot 0.7H_2O$ (calcd. H 2.92, Al 8.29, N 4.30, Ni 32.62; found H 3.01, Al 8.15, N 4.23, Ni 33.49).

Figure 2A shows the Ni K-edge $k^1\chi(k)$ spectrum and Fourier transform magnitude of the powdered NiAl-NO_3-LDH, while Figure 2B displays the experimental (solid) and fitted (dotted) EXAFS curves with k^1-weight for Ni–O coordination in the powdered NiAl-NO_3-LDH. The fitting parameters are listed in Table 1 [$Ni(OH)_2$ was used as a reference sample]. Data analysis suggests a Ni–O distance of 2.04 Å and a Ni–O coordination number (CN_{Ni-O}) of six

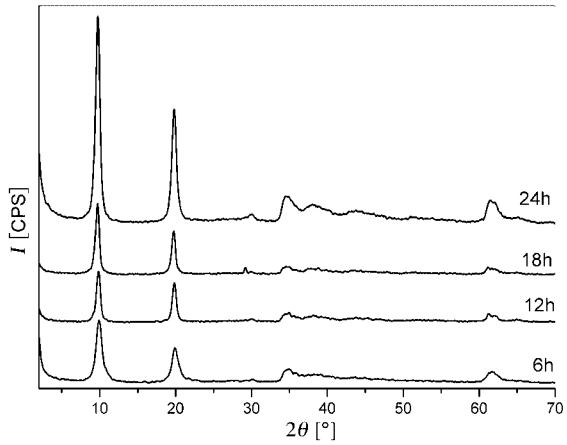

Figure 1. Powder XRD patterns of NiAl-NO_3-LDHs with different aging times at 180 °C.

for the NiAl-NO_3-LDH, which corresponds well to the data reported by Scheidegger et al.[21] This reveals that the first coordination shell of Ni comprises six oxygen atoms at 2.04 Å, indicating that Ni^{II} is coordinated in an octahedral environment.

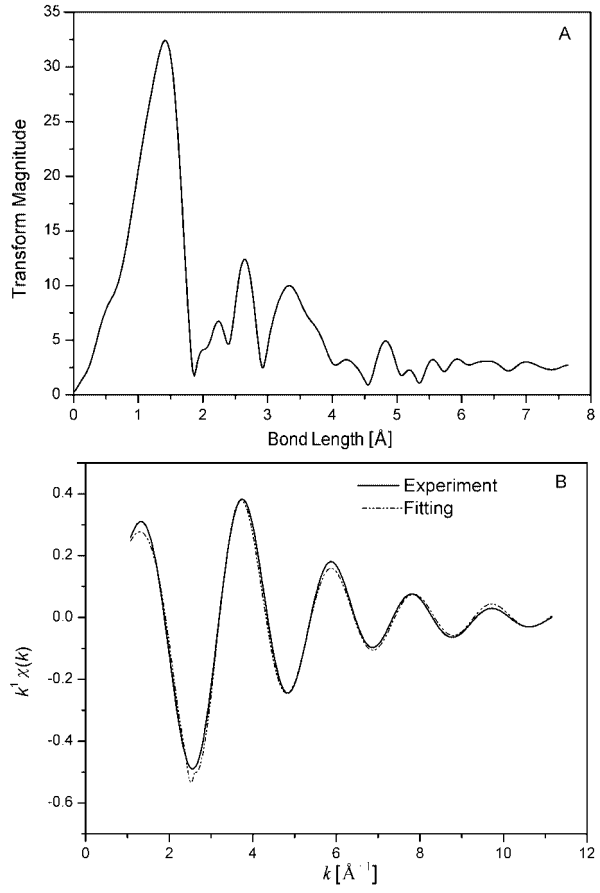

Figure 2. (A) Ni *K*-edge $k^1\chi(k)$ spectrum and Fourier transform magnitude of powdered NiAl-NO_3-LDH. (B) Experimental (solid line) and fitted (dotted line) EXAFS curves with k^1-weight for Ni–O coordination in powdered NiAl-NO_3-LDH.

Table 1. Local coordination parameters around Ni in powdered NiAl-NO_3-LDH.

Sample	CN_{Ni-O}	R_{Ni-O} [Å]	σ^2_{Ni-O} [Å]^2
$Ni(OH)_2$	6.0	2.05	0.002
NiAl-NO_3-LDH	6.0	2.04	0.003

Photochromism in NiAl-NO_3-LDHs

Photochromism in NiAl-NO_3-LDHs has been observed for the first time in this work. Figure 3c shows the UV/Vis absorption spectra of NiAl-NO_3-LDH both before and after UV irradiation. For the as-synthesized NiAl-NO_3-LDH sample before UV irradiation, two absorption peaks (at ca. 376 and 652 nm) were observed, which were assigned to the (d–d) spin-allowed electronic transitions expected for a Ni^{2+} ion in an octahedral crystal field.[22] Upon irradiation of NiAl-NO_3-LDH with UV light, the green samples rapidly turned black. Furthermore, there was a remarkable enhancement of absorption in the wavelength range 300–650 nm (Figure 3c). No change in color could be observed, even when the black-colored NiAl-NO_3-LDH was kept at room temperature for a week. However, upon heating to 70 °C for 2 h, the color returned to green. The UV/Vis absorption spectrum also recovered its original profile (dotted line shown in Figure 3c, almost coincident with the initial spectrum), demonstrating the reversibility of the photochromism. Moreover, both the reversibility and reproducibility of the photochromism were investigated. The inset in Figure 3 displays the UV absorbance of this material at 500 nm, before and after ten irradiation cycles, indicating a rather high reversibility and reproducibility.

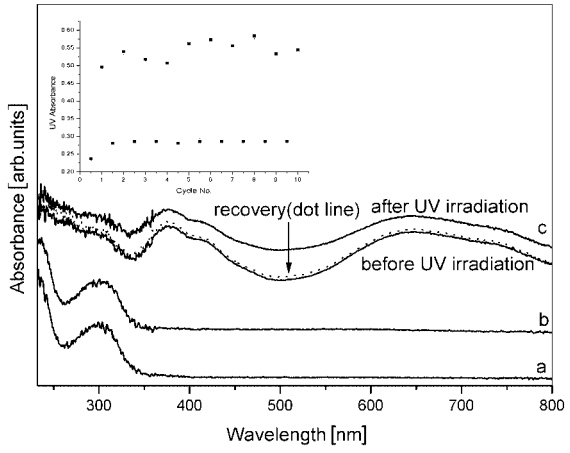

Figure 3. UV/Vis absorption spectra of (a) MgAl-NO_3-LDH, (b) ZnAl-NO_3-LDH and (c) NiAl-NO_3-LDH, before and after UV irradiation [absorption curves of before and after UV irradiation for (a) and (b) are coincident]. Inset: the relationship between the UV absorbance of NiAl-NO_3-LDH at 500 nm (before and after irradiation) and cycle number.

The Photochromic Mechanism in NiAl-NO_3-LDHs

Influence of Nickel Ions

In order to study the effect of the nickel ions of the host layers on photochromic behavior, MgAl-NO_3-LDH and

ZnAl-NO_3-LDH were prepared as samples for comparison. All three samples exhibit a PXRD pattern characteristic of LDH-like materials, and the interlayer distance of the three intercalates is about 0.88 nm, indicating well-defined LDHs containing nitrate anions.

Figure 3 displays the UV/Vis absorption spectra of the three samples, both before and after UV irradiation. No obvious change could be observed in the spectra of MgAl- and ZnAl-NO_3-LDHs after UV-light irradiation (Figure 3a and Figure 3b, respectively). This observation is in agreement with their invariable white color, and in contrast with the photochromic behavior that was observed in the case of NiAl-NO_3-LDH, as described above. This indicates that the nickel ions in the host layer play an important role in the photochromic behavior. This is possibly related to the octahedral coordination environment of the nickel ion.

Influence of Aging Conditions

Figure 1 and Figure 4 display the PXRD patterns of NiAl-NO_3-LDHs with different aging times and aging temperatures, respectively. All nine samples exhibit a PXRD pattern characteristic of LDH-like materials, with an interlayer distance of approximately 0.89 nm. It can be seen from Figure 1 and Figure 4 that the reflection intensity of the LDHs becomes stronger with an increase in the aging time or aging temperature. The indexing parameters are listed in Table 2. It should be noted that there is a decrease in the half-peak-width parameter, and an increase in the crystallite size in the *c* direction, upon increasing aging time or temperature. This is an indication that the stacking sequences of the LDHs become more ordered and higher crystallinity is obtained with increasing aging time or temperature.

Figure 5A and Figure 6A show the UV/Vis absorption spectra of powdered NiAl-NO_3-LDHs with different aging times and temperatures, respectively, both before and after UV irradiation. On irradiation the samples prepared with a 6 h aging time, or at 70 °C aging temperature, show the most remarkable enhancement of absorption in the wavelength range 300–650 nm. They are also accompanied by

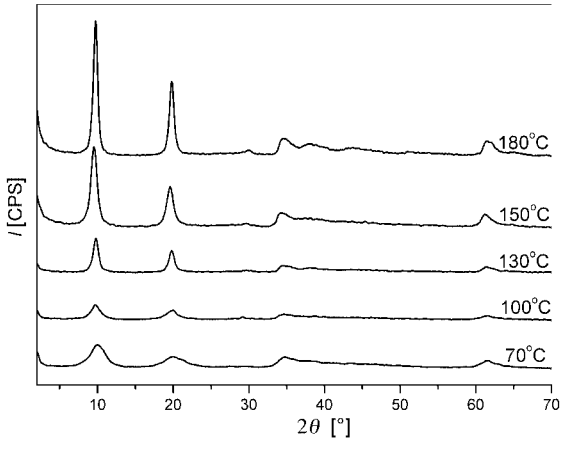

Figure 4. Powder XRD patterns of NiAl-NO_3-LDH aged for 24 h at different aging temperatures.

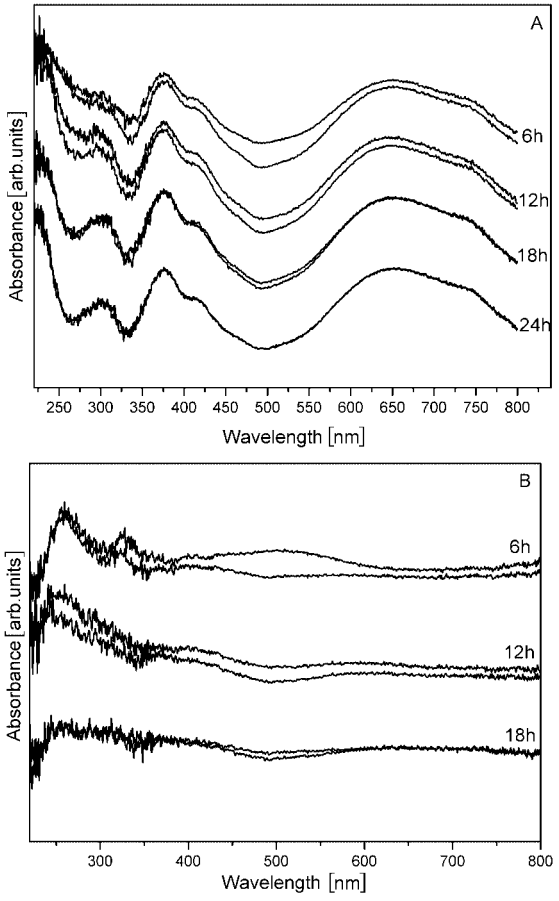

Figure 5. (A) UV/Vis absorption spectra of NiAl-NO_3-LDHs with different aging times at 180 °C, before and after UV irradiation. (B) Background correction for the absorption spectra of the NiAl-NO_3-LDHs from (A) before and after UV irradiation.

Table 2. Lattice parameters of NiAl-NO_3-LDHs prepared under different conditions.

Parameters	Samples with different aging temperatures					Samples with different aging times			
	70 °C	100 °C	130 °C	150 °C	180 °C	6 h	12 h	18 h	24 h
d_{003} [nm]	0.879	0.904	0.927	0.903	0.906	0.893	0.900	0.912	0.906
half-peak width of the 003 reflection [°]	1.810	1.270	0.933	0.808	0.515	0.866	0.613	0.583	0.515
d_{110} [nm]	0.151	0.151	0.151	0.151	0.151	0.150	0.151	0.152	0.151
lattice parameter *a* [nm][a]	0.302	0.302	0.302	0.302	0.302	0.300	0.302	0.304	0.302
lattice parameter *c* [nm][b]	2.637	2.712	2.781	2.709	2.718	2.679	2.700	2.736	2.718
crystallite size in *c* direction [nm][c]	4.361	6.215	8.458	9.768	15.32	9.115	12.88	13.54	15.32

[a] $a = 2d_{110}$. [b] $c = 3d_{003}$. [c] Value calculated from the Scherrer equation.

the most obvious change in sample color, which indicates the most significant photochromism. Moreover, the enhancement of the absorption in the range 300–650 nm decreased upon increasing aging time or temperature. As the aging time was increased to 24 h, or the aging temperature was increased to 180 °C, no change could be observed in either the absorption spectra or the sample color following UV-light irradiation, which implied the absence of photochromic behavior. On the basis of the PXRD characterization above, it can be concluded that the ordered stacking sequences and the crystallinity of NiAl-NO_3-LDH have a marked influence on its photochromism. Moreover, the effect of the wavelength of the excitation light has been studied, and it was found that UV light with a wavelength below 376 nm could cause photochromism in the material.

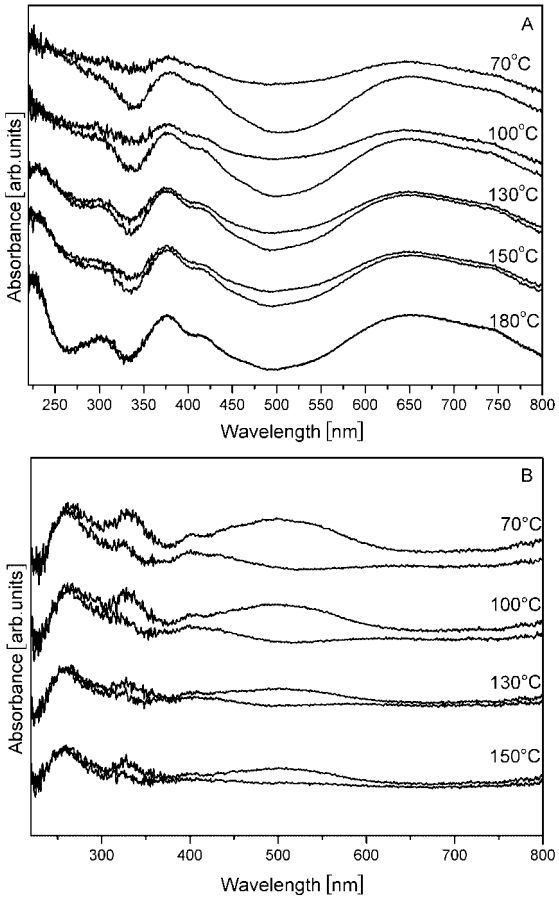

Figure 6. (A) UV/Vis absorption spectra of NiAl-NO_3-LDHs with different aging temperatures and aged for 24 h, before and after UV irradiation. (B) Background correction for the absorption spectra of the NiAl-NO_3-LDHs from (A) before and after UV irradiation.

In order to gain direct insight into photochromism in NiAl-NO_3-LDH, the NiAl-NO_3-LDH samples which were nonphotochromic (aging time 24 h and aging temperature 180 °C) were used as the baseline reference for further analysis of the UV/Vis spectra. Background correction was performed by subtracting the absorption spectrum of the nonphotochromic sample from the photochromic NiAl-NO_3-LDH samples, both before and after UV irradiation. The results are shown in Figure 5B and Figure 6B. Comparing the UV/Vis absorption spectra before and after UV irradiation, it can be seen that there is an obvious peak at approximately 500 nm. This indicates that there might be some specific structural unit, with Ni in an octahedrally coordinated environment, which results in photochromism in NiAl-NO_3-LDH. As the aging time or temperature increases, the stacking sequences of the LDHs become more ordered, leading to the loss of the specific structural unit and thus to the loss of photochromic behavior.

Influence of Host–Guest Interactions

In order to study the influence of host–guest interactions, two samples of NiAl-CO_3-LDH were prepared: one by the ion-exchange method from a NiAl-NO_3-LDH precursor and the other by direct coprecipitation. Both samples exhibit a PXRD pattern characteristic of LDH-like materials, with an interlayer distance of approximately 0.76 nm, indicating well-defined LDHs containing carbonate anions. Figure 7 displays a comparison of the FTIR spectra of the two NiAl-CO_3-LDH samples. Both show the strong, sharp band at approximately 1363 cm^{-1} due to the absorption of interlayer carbonate anions. However, it can be seen that a peak at approximately 1384 cm^{-1} was observed in the sample prepared by ion-exchange (Figure 7a), which indicates the presence of a small amount of nitrate anions.

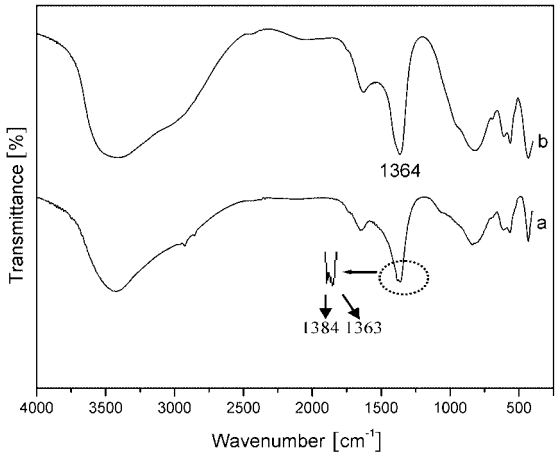

Figure 7. FTIR spectra of NiAl-CO_3-LDHs prepared by (a) ion exchange and (b) coprecipitation.

On the basis of elemental analysis, the chemical composition of the NiAl-CO_3-LDH that was prepared by coprecipitation was found to be $[Ni_{0.656}Al_{0.344}(OH)_2](CO_3^{2-})_{0.172}\cdot 0.8H_2O$ (calcd. C 2.06, H 3.37, Al 8.70, Ni 36.27; found C 2.12, H 3.31, Al 8.73, Ni 36.19). However, the chemical composition of the NiAl-CO_3-LDH that was prepared by the ion-exchange method from a NiAl-NO_3-LDH precursor was found to be $[Ni_{0.647}Al_{0.353}(OH)_2](CO_3^{2-})_{0.151}(NO_3^{-})_{0.051}\cdot 0.7H_2O$ (calcd. C 1.70, H 3.19, Al 8.95, N 0.67, Ni 35.83; found C 1.62, H 3.13, Al 8.86, N 0.71, Ni 35.76). It can be seen that the sample prepared by coprecipitation was a pure CO_3^{2-} LDH, while the other one, prepared by ion-exchange from a NiAl-NO_3-LDH precursor, contained both CO_3^{2-} and a little unexchangeable NO_3^{-}.

Figure 8a and b show the UV/Vis absorption spectra of the two powdered NiAl-CO_3-LDH samples before and after UV irradiation. It was found that almost no change in the absorption spectrum, after UV-light irradiation, could be observed for the NiAl-CO_3-LDH prepared by coprecipitation (Figure 8b), which means that photochromism is not an intrinsic property of NiAl-CO_3-LDHs. However, in the case of the sample prepared by ion exchange, a considerable enhancement in the 300–650 nm range (Figure 8a) was observed after UV irradiation. This is an indication that the interaction between Ni^{2+} and co-intercalated nitrate anions is indispensable for the photochromism in NiAl-CO_3-LDHs prepared by ion exchange. This is possibly related to the remaining nitrate anions that interact strongly with Ni^{2+} ions in NiAl-NO_3-LDHs through chemical bonding and thus cannot be exchanged by CO_3^{2-}.

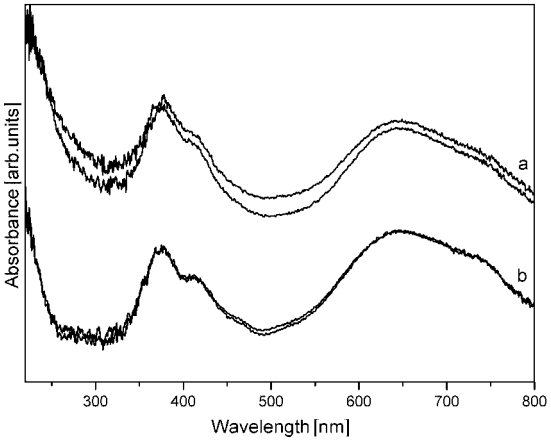

Figure 8. UV/Vis absorption spectra of powdered NiAl-CO_3-LDHs, both before and after UV irradiation, prepared by (a) ion exchange and (b) coprecipitation.

XPS Data

In order to confirm whether the photochromic behavior of NiAl-NO_3-LDHs is related to the redox of Ni^{2+}, XPS was used to determine the chemical environment of Ni, N, and O before and after UV irradiation. The XPS Ni2$p_{3/2}$, N1s, and O1s core level spectra of NiAl-NO_3-LDHs, before and after UV irradiation, are shown in Figure 9. The binding energy (BE) value of the main Ni2$p_{3/2}$ peak, at around 856.4/856.5 eV, is assigned to the Ni^{2+} ion by comparison with the known BE value for Ni2$p_{3/2}$ photoelectrons in $Ni(OH)_2$ (855.6–856.6 eV).[23] The XPS N1s peak at around 406.6/406.7 eV is attributed to N^{5+} from the nitrate anions, and the XPS O1s peak at around 531.9/531.8 eV is due to O^{2-} from the nitrate anions. As no remarkable change in the values of the BE can be observed after UV irradiation, it is reasonable to deduce that the oxidation states of Ni, N, and O in NiAl-NO_3-LDHs do not change, and hence a mechanism based on the redox of Ni^{2+} can be excluded.

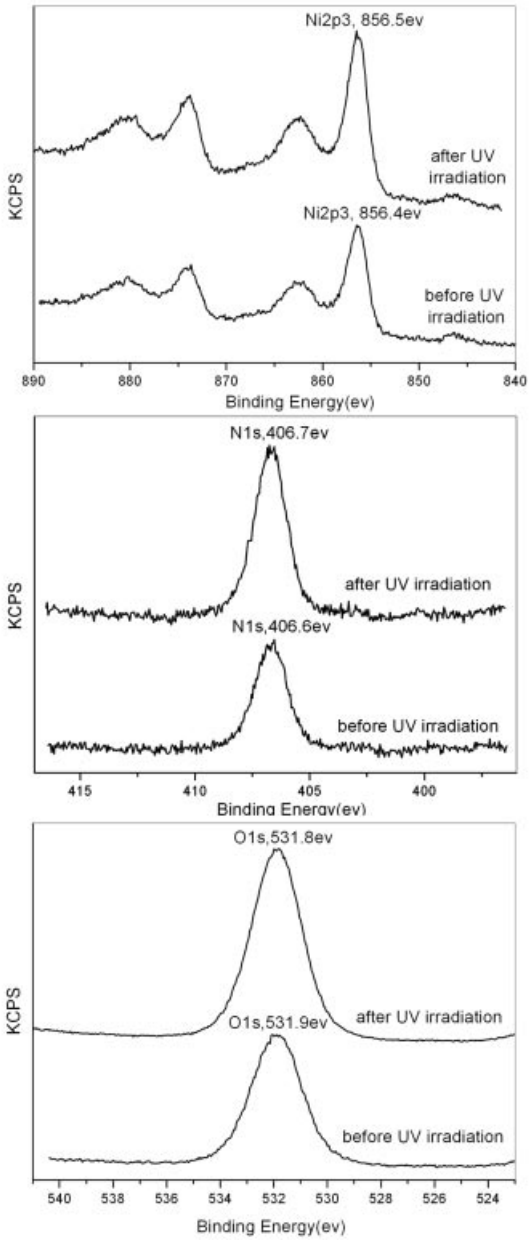

Figure 9. XPS spectra of Ni2$p_{3/2}$, N1s, and O1s for NiAl-NO_3-LDHs before and after UV irradiation.

ESR Data

ESR was used to study the coordination environment of Ni^{2+} in NiAl-NO_3-LDHs to obtain a further understanding of the photochromic mechanism. It has been reported that Ni^{2+} ions in $Ni(OH)_2$ are ESR silent at room temperature, most probably because of the regular octahedral crystal field.[22] Figure 10 displays the ESR spectra of powdered NiAl-NO_3-LDH before and after UV irradiation, as well as that of NiAl-CO_3-LDH prepared by coprecipitation, as a reference sample. It can be seen from Figure 10a that NiAl-CO_3-LDH is ESR silent at room temperature and at liquid nitrogen temperature, because of its Ni–OH regular octahedral crystal field. However, in the case of NiAl-NO_3-LDH, distinct signals with g = 2.163 (Figure 10b) and g = 2.643

(Figure 10c) were observed for the sample before and after UV irradiation, respectively. These can be attributed to Ni^{2+} ions ($3d^8$ electronic configuration) in a strongly distorted octahedral crystal field.[22] The difference in the *g* values indicates that the distortion in the octahedral crystal field for NiAl-NO_3-LDH is not completely the same before and after UV irradiation.

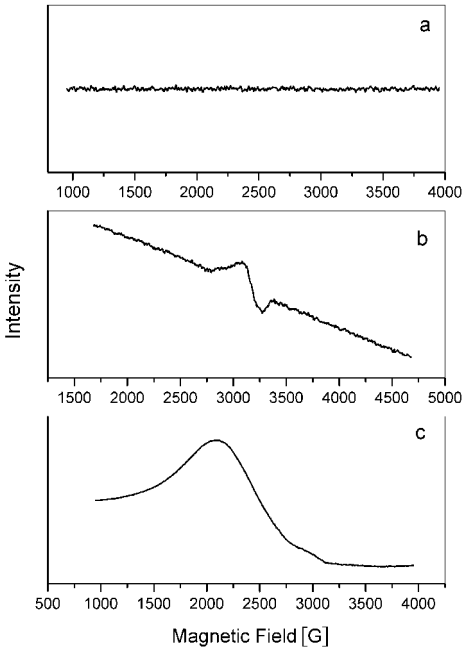

Figure 10. ESR spectra of powdered NiAl-CO_3-LDH prepared by coprecipitation (a), and NiAl-NO_3-LDHs before irradiation (b) and after irradiation (c).

On the basis of the discussion above, it can be concluded that the host–guest interaction between Ni^{2+} and the nitrate anions, and thus the presence of the specific octahedral crystal field of the Ni^{2+}, leads to photochromism in NiAl-NO_3-LDHs. Single-crystal structure analysis of CaAl-NO_3/CO_3/SO_4/Cl-LDHs has revealed that Ca^{2+} ions are sevenfold coordinated by O atoms. A water molecule, a carbonate anion, or a nitrate anion occupies the seventh coordination site of three of the four Ca^{2+} ions contained in the main layer.[24–27] Moreover, Steven et al. reported that, in the layered material $Ni_2(OH)_3NO_3$, the nitrate anion was located in the interlayer region and was coordinated through one oxygen atom directly to the matrix Ni^{2+} cation.[28] In the current study, taking into account the confirmation by EXAFS data that Ni^{2+} ions are sixfold coordinated (Table 1), the evidence from ESR data that Ni^{2+} ions exist in a distorted octahedral crystal field, and the presence of unexchangeable NO_3^-, it can be concluded that there are specific units of octahedral structure in which Ni^{2+} is coordinated by five hydroxy groups and one nitrate anion through the O atom in NiAl-NO_3-LDH, as shown in Figure 11. The influence of water cannot be excluded completely, and there is the possibility that a hydrogen-bonding system exists between the host hydroxy and nitrate anions, and water molecules, and thus water has a secondary influence on the photochromism of NiAl-NO_3-LDH (as shown in Figure 11). Further studies on the effects of water, as well as theoretical calculations, are under investigation at our laboratory.

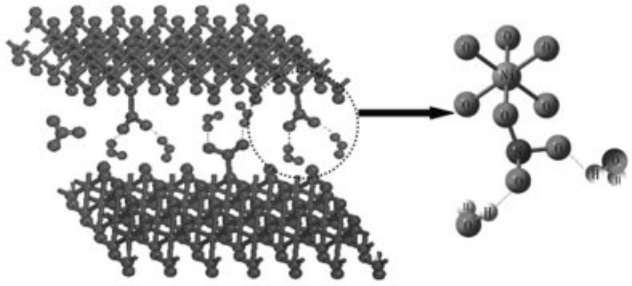

Figure 11. Schematic representation of the structure of NiAl-NO_3-LDH.

The electronic configuration of Ni^{2+} ions in the ground state is $3d^8$ ($t_{2g}^6e_g^2$). As shown in Figure 12a, the octahedral crystal field of the Ni^{2+} ions is generated by the coordinated O atom of the nitrate anion, and is somewhat distorted with a *g* value of 2.163, derived from ESR spectroscopy data. Under UV-light irradiation, the electronic configuration of the Ni^{2+} ions in the excited state is $3d^8$ ($t_{2g}^5e_g^3$), which speaks in favor of the Jahn–Teller effect, and thus leads to a more strongly distorted octahedral crystal field (Figure 12b). The latter structure is quite stable at room temperature and cannot revert spontaneously. In comparison with the sample before UV irradiation, it demonstrates changes in the UV/Vis absorption spectrum (especially the strong absorption enhancement in at a wavelength of 500 nm) and in the *g* value determined by ESR spectroscopy (from 2.163 to 2.634). Upon heating, the radiation-induced structure recovers its original state, and the color changes from black to green. Because the distorted octahedral structure [$Ni(OH)_5NO_3$] was a metastable state thermodynamically, it reverted to the stable regular octahedral unit [$Ni(OH)_6$] by substitution of the NO_3^- by an OH^- group upon increasing aging time or temperature during the preparation process. As a result, the specific octahedral crystal field of the Ni^{2+} ion, coordinated by a nitrate anion, leads to photochromism in NiAl-NO_3-LDHs.

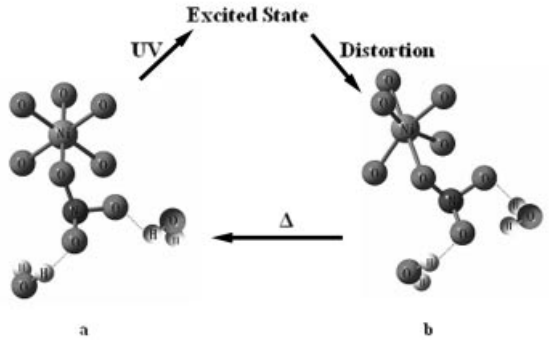

Figure 12. Photochromic mechanism in NiAl-NO_3-LDH: (a) structure before UV irradiation and (b) structure after UV irradiation.

Conclusions

Photochromism in NiAl-NO_3-LDHs has been studied in this work. The crystalline structure and chemical composition of NiAl-NO_3-LDHs have been characterized on the basis of the results of PXRD, FTIR, EXAFS, and elemental analysis. The studies on the influence of aging conditions indicate that the host–guest interaction between the nickel ion in the host layer and the interlayer NO_3^- plays an important role in its photochromic behavior. Taking into account the confirmation by EXAFS data that the Ni^{2+} ions are sixfold coordinated, the ESR spectroscopy data that indicates that Ni^{2+} is ESR active in NiAl-NO_3-LDHs, the confirmation of the presence of some unexchangeable NO_3^-, and the exclusion of the redox of Ni^{2+}, it can be concluded that there is a specific unit of distorted octahedral structure. This unit consists of a Ni^{2+} ion, which is coordinated by O atoms from five hydroxy groups and one nitrate anion, and results in photochromism in NiAl-NO_3-LDHs.

Experimental Section

Preparation of NiAl-NO_3-LDH: NiAl-NO_3-LDH was synthesized by a hydrothermal method.[29] Typically, an aqueous solution of NaOH (24 g, 0.6 mol) in deionized water (40 mL) was added dropwise to a vigorously stirred, freshly prepared solution containing $Ni(NO_3)_2{\cdot}6H_2O$ (58.156 g, 0.2 mol) and $Al(NO_3)_3{\cdot}9H_2O$ (37.513 g, 0.1 mol) (Ni^{2+}/Al^{3+} = 2) in deionized water (100 mL) under a nitrogen atmosphere at room temperature. The final pH was approximately 6. The suspension was transferred to a Teflon-lined autoclave and heated at 70, 100, 130, 150, or 180 °C for a specific time. The solid precipitate was collected by filtration through a membrane filter under suction, washed thoroughly with water, and dried at 70 °C for 18 h.

Preparation of MgAl-NO_3-LDH and ZnAl-NO_3-LDH: MgAl-NO_3-LDH and ZnAl-NO_3-LDH, which were used as comparison samples, were synthesized by a hydrothermal method. MgAl-NO_3-LDH was synthesized by a procedure similar to that described previously.[30] A solution of $Mg(NO_3)_2{\cdot}6H_2O$ (32.0 g, 0.125 mol) and $Al(NO_3)_3{\cdot}9H_2O$ (11.7 g, 0.062 mol) in deionized water (200 mL) was added dropwise over 2 h to a solution of NaOH (12.5 g, 0.310 mol) and $NaNO_3$ (18.2 g, 0.210 mol) in water (250 mL). The mixture was transferred to a Teflon-lined autoclave and heated at 70 °C for 24 h. The precipitate was separated by centrifugation, washed with water, and dried at 70 °C for 18 h. ZnAl-NO_3-LDH was obtained by a similar method.

Preparation of NiAl-CO_3-LDH: NiAl-CO_3-LDH was prepared by both coprecipitation and ion exchange. The sample prepared by the coprecipitation method was synthesized according to a literature procedure.[31] In the case of the NiAl-CO_3-LDH sample obtained by ion exchange, the precursor NiAl-NO_3-LDH was synthesized first by the procedure described above. Subsequently, a solution of Na_2CO_3 in deionized water (50 mL) was added to a suspension of NiAl-NO_3-LDH in water (50 mL), and the mixture was then heated to 70 °C for 24 h. The product was washed extensively with deionized water, centrifuged, and dried at 70 °C for 18 h.

Characterization Techniques

PXRD patterns were obtained by using a Shimadzu XRD-6000 diffractometer under the following conditions: Cu-K_α radiation (λ = 1.542 Å, 2θ = 2–70°), 40 kV, 30 mA. Infrared spectra of samples were recorded by using a Bruker Vector 22 FTIR spectrometer. Specimens were prepared as KBr pellets. Elemental analysis of the metal content was performed with an ICPS-7500 inductively coupled plasma optical-emission spectrometer. C, H, and N elemental analysis was carried out with an Elementar Vario elemental analyzer. The ESR spectra were recorded at room temperature with a Bruker ESP300 spectrometer. A standard 100 MHz field modulation and a 5–10 G modulation width were used. XPS was recorded with a VG Scientific ESCALab220i-XL (VG Scientific Ltd., UK) spectrometer.

The EXAFS spectrum around the Ni *K*-adsorption edge was obtained by using the beamline 4W1B of the Beijing Synchrotron Radiation Facility (BSRF). The NiAl-NO_3-LDH nanoparticles were homogeneously smeared on Scotch adhesive tape. More than eight layers were folded to reach the optimum absorption thickness. The X-ray absorption spectrum of the Ni *K*-edge of NiAl-NO_3-LDH was collected at ambient temperature in the transmission mode. The storage ring was operated at 2.2 GeV with a typical current of 50 mA. Fixed-exit Si(111) flat double crystals were used as a monochromator. The incident and transmission X-ray intensities were detected by using ion chambers installed in front of and behind the sample. The X-ray energy was calibrated by using the Ni *K*-absorption edge (8348 eV). The absorption spectrum was collected from 200 eV below the absorption threshold to over 700 eV above the threshold.

EXAFS data reduction was performed by using WinXAS 97 1.1 and following standard procedures. The first maximum of the first derivative of the absorption edge was chosen as the energy threshold. The pre-edge absorption background was fitted and subtracted by using a linear function. A derivative method was used to derive the EXAFS signal and remove the post-edge absorption background. EXAFS functions were normalized by using the absorption-edge jump and were Fourier-transformed to *R* space with k^1-weight in the range 1.1–11.3 Å. Fourier filters were used in the range 0.3–1.8 Å. Theoretical scattering paths for the fit were calculated by using the structures of α-$Ni(OH)_2$. To reduce the number of adjustable parameters, the amplitude reduction factor, S_0^2, was fixed at 1.1. The $R_{Ni–O}$ values are estimated to be accurate to 0.02 Å, and the ΔE_0 and $CN_{Ni–O}$ values are estimated to be accurate to 20%. The accuracy estimates are based on the results of theoretical fits to the spectra of the reference compounds of known structure.

Study of the Photochromic Properties of LDHs: UV irradiation was carried out by using a 500-W xenon lamp. Absorption spectra were recorded by using a UV/Vis spectrophotometer (Shimadzu UV-2501 PC).

Acknowledgments

This project was supported by the National Natural Science Foundation Key Project of China (Project No.: 90306012), the National Basic Research Program (973 Program) (Project No.: 2004CB720602), the Ministry of Education Science and Technology Research Project of China (Project No.: Key 104239), the Beijing Nova Program (No.: 2004A13), and the Program for Changjiang Scholars and Innovative Research Team in University (PCSIRT). We also acknowledge the Beijing Synchrotron Radiation Facility (BSRF) for provision of synchrotron radiation facilities and thank Dr. Yaning Xie and Tao Liu for assistance in using beamline 4W1B.

[1] M. Meyn, K. Beneke, G. Lagaly, *Inorg. Chem.* **1990**, *29*, 5201–5207.
[2] G. A. Caravaggio, C. Detellier, Z. Wronski, *J. Mater. Chem.* **2001**, *11*, 912–921.
[3] A. Corma, V. Fornes, F. Rey, A. Cervilla, E. Llopis, A. Ribera, *J. Catal.* **1995**, *152*, 237–242.
[4] M. Ogawa, K. Kuroda, *Chem. Rev.* **1995**, *95*, 399–438.
[5] H. Tagaya, A. Ogata, T. Kuwahara, S. Ogata, M. Karasu, J. I. Kadokawa, J. Chiba, *Microporous Mater.* **1996**, *7*, 151–158.
[6] B. Sels, D. De Vos, M. Buntinx, F. Pierard, A. Kirsch-De Mesmaeker, P. Jacobs, *Nature* **1999**, *400*, 855–857.
[7] L. Ukrainczyk, M. Chibwe, T. J. Pinnavaia, S. A. Boyd, *Environ. Sci. Technol.* **1995**, *29*, 439–445.
[8] A. M. Fogg, V. M. Green, H. G. Harvey, D. O'Hare, *Adv. Mater.* **1999**, *11*, 1466–1469.
[9] A. M. Fogg, J. S. Dunn, S. G. Shyu, D. R. Cary, D. O'Hare, *Chem. Mater.* **1998**, *10*, 351–355.
[10] A. I. Khan, L. Lei, A. J. Norquist, D. O'Hare, *Chem. Commun.* **2001**, 2342–2343.
[11] V. Ambrogi, G. Fardella, G. Grandolini, L. Perioli, *Int. J. Pharm.* **2001**, *220*, 23–32.
[12] P. V. Kamath, M. Dixit, L. Indira, A. K. Shukla, V. G. Kumar, N. Munichandraiah, *J. Electrochem. Soc.* **1994**, *141*, 2956–2959.
[13] A. Sugimoto, S. Ishida, K. Hanawa, *J. Electrochem. Soc.* **1999**, *146*, 1251–1255.
[14] J. C. Crano, T. Flood, D. Knowles, A. Kumar, B. Van Gemert, *Pure Appl. Chem.* **1996**, *68*, 1395–1398.
[15] J. M. Lehn, *Supramolecular Chemistry*, VCH, Weinheim, **1995**, p. 105.
[16] F. Vogtle, *Supramolekulare Chemie*, Teubner, Stuttgart, **1992**, ch. 7.
[17] J. Peretti, J. Biteau, J. P. Boilot, F. Chaput, V. I. Safarov, J. M. Lehn, A. Fernandez-Acebes, *Appl. Phys. Lett.* **1999**, *74*, 1657–1659.
[18] K. Schaffner, S. E. Braslavsky, A. R. Holzwarth, *Adv. Photochem.* **1990**, *15*, 229–277.
[19] H. Tagaya, T. Kuwahara, S. Sato, J. I. Kadokawa, M. Karasu, K. Masa, K. Chiba, *J. Mater. Chem.* **1993**, *3*, 317–318.
[20] H. Tagaya, S. Sato, T. Kuwahara, J. I. Kadokawa, K. Masa, K. Chiba, *J. Mater. Chem.* **1994**, *4*, 1907–1912.
[21] A. M. Scheidegger, E. Wieland, A. C. Scheinost, R. Dahn, P. Spieler, *Environ. Sci. Technol.* **2000**, *34*, 4545–4548.
[22] A. Davidson, J. F. Tempere, M. Che, *J. Phys. Chem.* **1996**, *100*, 4919–4929.
[23] P. Dufresne, E. Grimblot, J. P. Bonnelle, *J. Phys. Chem.* **1981**, *85*, 2344–2351.
[24] A. Tersis, S. Filippakis, H. J. Kuzel, H. Burzlaff, *Z. Kristallogr.* **1987**, *181*, 29–34.
[25] R. Allmann, J. Neues, *Neues Jahrb. Mineral. Monatsh.* **1977**, *3*, 136–144.
[26] M. Francois, G. Renaudin, O. Evrard, *Acta Crystallogr. Sect. A* **1998**, *54*, 1214–1217.
[27] G. Renaudin, M. Francois, *Acta Crystallogr. Sect. A* **1999**, *55*, 835–838.
[28] P. N. Steven, J. William, *J. Solid State Chem.* **1999**, *148*, 26–40.
[29] F. Prinetto, D. Tichit, R. Teissier, B. Coq, *Catal. Today* **2000**, *55*, 103–116.
[30] J. H. Lee, S. W. Rhee, D. Y. Jung, *Chem. Mater.* **2004**, *16*, 3774–3779.
[31] F. Kooli, K. Kosuge, A. Tsunashima, *J. Solid State Chem.* **1995**, *118*, 285–291.

Received: January 20, 2006
Published Online: May 9, 2006

